RESEARCH ARTICLE

Macromolecular Materials and Engineering
www.mame-journal.de

Photocurable Methacrylated Silk Fibroin/Hyaluronic Acid Dual Macrocrosslinker System Generating Extracellular Matrix-Inspired Tough and Stretchable Hydrogels

Berkant Yetiskin, Burak Tavsanli, and Oguz Okay*

Extracellular matrix (ECM) containing interconnected proteins and glycosaminoglycans (GAGs) is a vital component of a tissue. Its gel-like physicochemical architecture is always a model for scientists studying in the fields of material science. Here, inspired from the ECM, soft hydrogels possessing an interconnected protein/GAG network are fabricated. This network comprises silk fibroin (SF) and hyaluronic acid (HA) as a protein and a GAG component, respectively. The interconnection of the SF and HA is performed by using both methacrylated SF (meth-SF) and HA (meth-HA), which behave as macrocroslinkers for a monomer forming a flexible polymer network between the meth-SF and meth-HA. Meth-HA/meth-SF hydrogels can be compressed and stretched up to 95% and 300%, respectively, with fracture stresses varying between kPa to MPa ranges. Furthermore, they have highly frequency-dependent viscoelastic properties above a particular frequency, likewise seen in many cells and tissues. Mechanical and viscoelastic properties of the hydrogels can be easily tuned by changing the methacrylation degree of the HA, and the concentration and the type of the monomer. It is believed that the meth-HA/meth-SF hydrogels prepared within the scope of this study will be good candidates for tissue engineering applications.

1. Introduction

Cells and tissues are nature's life-sustaining gel-like soft materials that withstand significant mechanical stresses during the lifespan of a living creature. Their mechanical resilience and stability are based upon two viscoelastic composite networks, namely the skeleton and the ECM, located inside and outside of a cell, respectively, which are originated from interconnected biopolymers.[1] For instance, in the cytoskeleton, actin filaments are crosslinked by unique proteins such as α-actinin and fascin to generate a skeletal framework within the cell.[2,3] In the ECM, collagen, a glycine-rich fibrous structural protein that mainly found in connective tissues, is crosslinked through lysine residues via lysyl oxidase enzyme to form a highly stiff and elastic protein network, while GAGs such as HA, form a soft hydrogel with energy-dissipating properties on account of its capacity to hold water.[4,5] These evolutionary achieved synergic and hierarchical natural networks have always been a model for material scientists to fabricate mechanically robust and tough soft materials for tissue engineering, resilient electronics, soft robotics, and many other application areas.[6–9]

For tissue-mimicking synthetic soft materials, hydrogels are the best candidate beyond any doubt due to their tissue-like high water content as well as an elastic polymer network with adjustable physicochemical and mechanical properties.[10] However, hydrogels synthesized by traditional methods are generally fragile and brittle in compression and tension.[11,12] This is the main reason for the exponential increase seen in research focusing on the reinforcing of the mechanical properties of the hydrogels. Such studies have been constitutively related to creating an efficient mechanical energy dissipation mechanism within the gel network by using different approaches.[13–16] Among them, interpenetrating gel networks integrating various kinds of polymers in a body, just as shown in the tissues, possess better mechanical and physical properties than the bare polymers individually, thus have drawn significant attention.[17]

Here, inspired by nature's interconnected gel architectures, we designed an interpenetrating gel network that simultaneously contains HA and a glycine-rich fibrous protein that can be crosslinked through the lysine residues, just as ECM. HA is a naturally occurring carbohydrate polymer consisting of disaccharide repeating units of β-1,4-D-glucuronic acid-β-1,3-N-acetyl-D-glucosamine.[18] Since the HA is one of the main components of the ECM, it has become an essential building block for creating new biomaterials for tissue engineering and regenerative medicine. On the other hand, we used SF as a protein component in our study, which is a high demanded biopolymer due to its high mechanical properties, biocompatibility,

B. Yetiskin, B. Tavsanli, O. Okay
Department of Chemistry
Istanbul Technical University
Maslak, Istanbul 34469, Turkey
E-mail: yetiskinb@itu.edu.tr
B. Tavsanli
Department of Chemistry
The University of Western Ontario
1151 Richmond Street, London, ON N6A 5B7, Canada

The ORCID identification number(s) for the author(s) of this article can be found under https://doi.org/10.1002/mame.202200334

DOI: 10.1002/mame.202200334

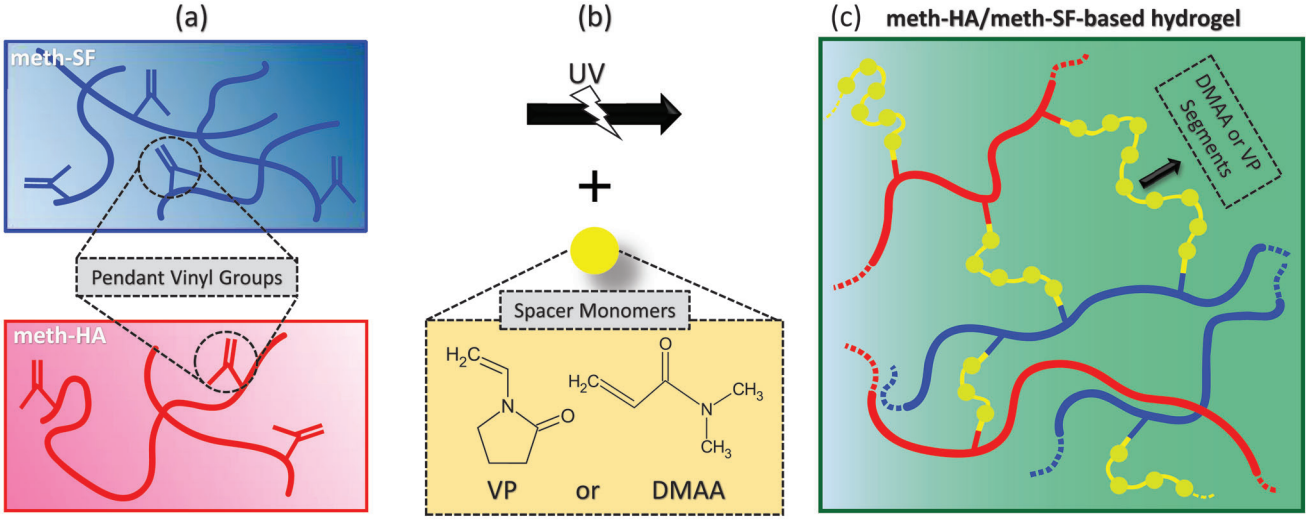

Figure 1. Schematically illustration of the preparation of a meth-HA/meth-SF hydrogel. a) Meth-HA and meth-SF chains containing pendant vinyl groups on their backbones. b,c) After addition of a monomer (VP or DMAA) acting as a spacer followed by a UV irradiation (b), a meth-HA/meth-SF-based hydrogel is formed (c). Blue and red lines represent the meth-SF and meth-HA chains, respectively, while yellow spheres indicate the monomer.

biodegradability, and easy processability.[19–22] SF/HA couple has been frequently researched for years, especially for tissue engineering applications, due to their biocompatibilities. However, their interconnection is generally carried out by using the EDC/NHS/MES ternary crosslinking system.[23–25]

One rational technique may be using methacrylated HA and SF simultaneously acting as a dual macrocrosslinker system by themselves (**Figure 1**). That is, in the present study, after the methacrylation of the HA and SF to obtain methacrylated HA and SF, that is, meth-HA and meth-SF, we prepared our composite hydrogels possessing high compressibility and stretchability up to 95% and 300%, respectively. Additionally, the methacrylation of the SF was provided via the lysine residues,[26,27] thus the hydrogels formed via the crosslinking through the lysine amino acids are good biomimetic materials for the ECM. The incorporation of the meth-HA and meth-SF into such mechanically stable viscoelastic gel form was accomplished by using monomers such as 1-vinyl-2-pyrrolidone (VP) or *N,N*-dimethylacrylamide (DMAA) acting as a spacer which generates highly elastic polymer chains that connected by meth-HA/meth-SF dual macrocrosslinker system. Even though the individual usage of the meth-HA and meth-SF as a macrocrosslinker for vinyl monomers was also reported previously by our research group,[27,28] their simultaneous application in this kind of perspective has not been reported yet until the present study, to our best knowledge.

Recently, meth-HA/meth-SF-based hydrogels obtained via photocuring have also been reported.[29,30] For instance, Wang et al. fabricated a series of meth-HA/meth-SF hydrogels for dental pulp regeneration.[29] Although these hydrogels can be compressed above 60% strain, their compressive fracture stresses are in kPa ranges.[29] Similarly, Ryoo et al. reported meth-HA/meth-SF hydrogels whose elastic modulus are below 1 kPa, which requires an ethanol treatment process to increase the mechanical properties.[30] However, we reported here meth-HA/meth-SF-based hydrogels in which meth-HA and meth-SF are used as macrocroslinkers for VP or DMAA monomers to create tough bioinspired interpenetrating gels. As will be discussed below, this strategy provides the fabrication of mechanically durable hydrogels having compressive fracture stresses in MPa ranges, stretchability, frequency-dependency, and so on.

In the present study, we first investigated the effects of the monomer type on the gelation mechanism and the main properties of the hydrogels, via the characterization of the hydrogels prepared in the absence and in the presence of a monomer (VP or DMAA), whose concentrations were first fixed at 3 w/v%. Then, after selecting a suitable monomer for the fabrication of tough hydrogels, that is, DMAA, we mainly studied meth-HA/meth-SF/DMAA hydrogels obtained at various DMAA concentrations. Consequently, as-prepared HA/SF-based hydrogels with high toughness may be a good candidate for the applications where biocompatibility and high mechanical performances are simultaneously required.

2. Results and Discussions

2.1. Gelation of the Meth-HA/Meth-SF System in the Presence and in the Absence of a Monomer: Formation of Meth-HA/Meth-SF-Based Hydrogels

To clarify the gelation efficiency, we first synthesized Series 1 and Series 2 hydrogels, that is, meth-HA/meth-SF hydrogels without (w/o) a monomer, and with (w/) a monomer (VP or DMAA) at a concentration of 3 w/v% respectively, then determined the gel fractions W_g of these hydrogels to understand the effects of the HA's methacrylation degree (MD) and the monomer type on the gelation. Similarly, Series 3 hydrogels were also fabricated by using DMAA monomer whose concentration was varied between 3 and 15 w/v% at all MD values. Thus, their W_g values were calculated to reveal the effect of the monomer concentration on the reaction yield. Furthermore, XRD measurements were also conducted for Series 3 hydrogels fabricated at the lowest and the

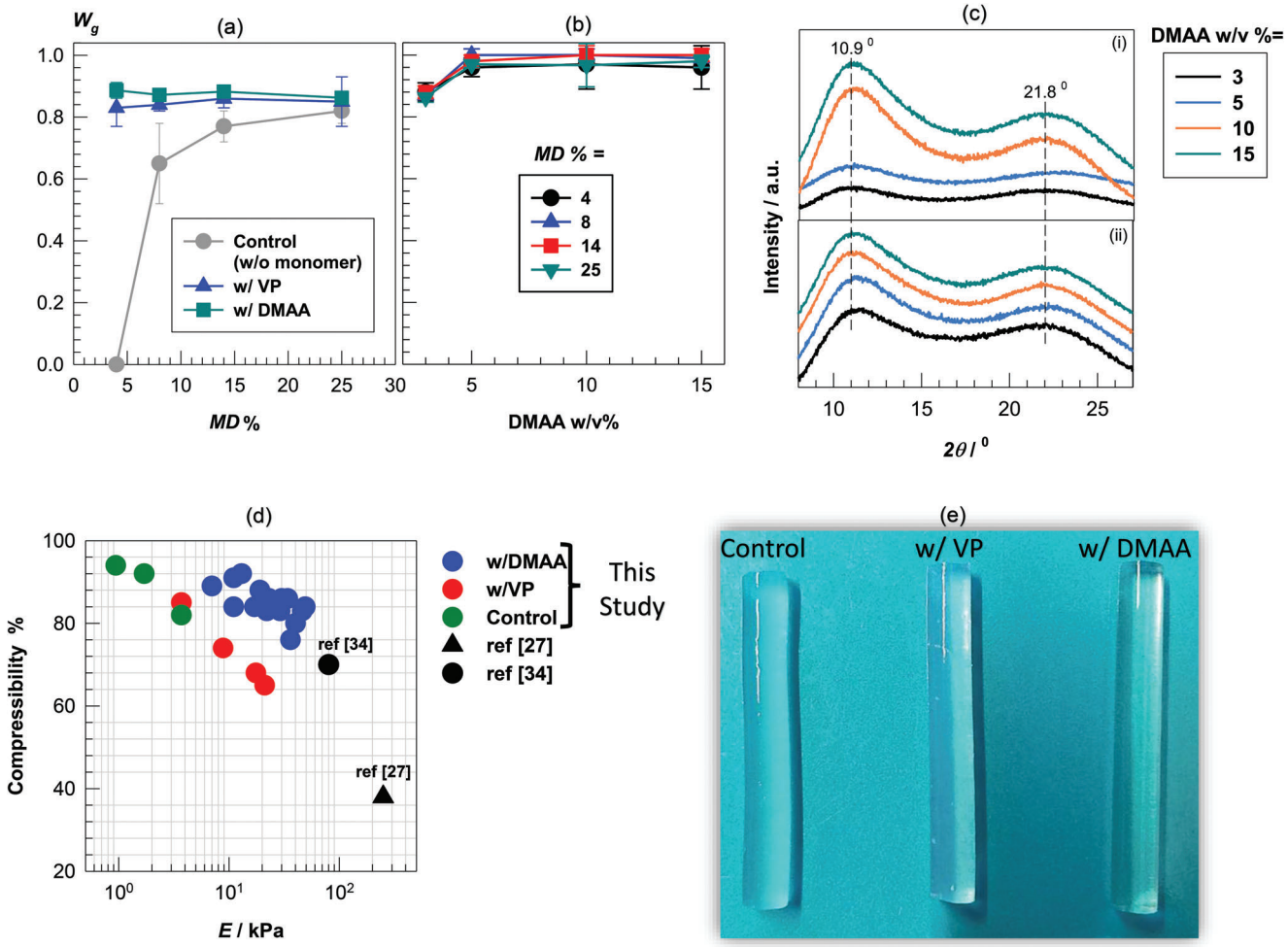

Figure 2. Gel fractions W_g of the hydrogels as a function of a) MD and b) DMAA concentration. c) XRD patterns of the hydrogels fabricated at various DMAA concentrations and at MD values of i) 4% and ii) 25%. d) Compressibility–Young's modulus (E) chart of the hydrogels fabricated in this study together with two references for comparison. e) Digital photographs of the hydrogels prepared in the absence of a monomer (control), and in the presence of VP (w/VP) and DMAA (w/DMAA) monomers, as indicated.

highest MD values, that is, 4% and 25%, to discuss the gelation mechanism with the perspective of β-sheet crystallites of the meth-SF. To fabricate Series 3 hydrogels, DMAA was chosen rather than the VP as also mentioned above, due to the mechanical performances of those materials, which will be discussed in the next section.

Figure 2a,b gives the W_g values of the hydrogels as a function of MD and DMAA concentration, respectively. A meth-HA/meth-SF hydrogel does not form at the lowest MD (4%) in the absence of a monomer (control, Figure 2a, grey symbols). However, when MD equals to 8%, 14%, and 25%, hydrogels can be obtained with a W_g of 0.65 ± 0.13, 0.77 ± 0.05, and 0.82 ± 0.04, respectively, indicating that the higher gelation yield is achieved with the increasing pendant vinyl group on the meth-HA chains.

On the other hand, even though a hydrogel did not occur at the lowest MD in the absence of a monomer, we were able to synthesize a hydrogel possessing a W_g of 0.83 ± 0.06 and above with the addition of a vinyl monomer (VP or DMAA at 3 w/v%) at this, and higher MD values (Figure 2a, blue and cyan symbols). This result may be explained by this theory: At the lowest MD, in which the amount of the pendant vinyl groups on the meth-HA backbone is minimum, they are not able to find each other to create a gel network, on account of the low mobility of the large molecules compared to small ones. However, the addition of a monomer as a spacer that in situ generates a polymer containing additional vinyl groups increases the possibility of the meth-HA and meth-SF chains to connect with each other through this polymer, as schematically illustrated in Figure 1c. Furthermore, when DMAA was chosen for the fabrication of the hydrogels at higher monomer concentrations (above 3 w/v%), W_g increased up to 1 at all MD values, indicating a full conversion from sol to gel state (Figure 2b).

Figure 2c gives the XRD patterns of the hydrogels fabricated at various DMAA concentrations, and at the lowest (4%, i) as well as at the highest (25%, ii) MD values. Due to the β-sheet crystallites of the SF protein, XRD patterns contain specific diffraction peaks at 2θ values of about 10° and 21°, whose intensity directly proportional to the β-sheet amount, that is, sharper and larger peaks indicate higher β-sheets. For instance, Oral et al. showed that the β-sheet ratio of the meth-SF is about 15% in sol state, and its XRD

pattern contains very broad peaks. However, after gelation, the β-sheet ratio increases up to 63 ± 1% while the diffraction peak at $2\theta = 21^{\circ}$ become significantly sharper.[27] Therefore, as the peaks shown in Figure 2c are broad and shallow, the β-sheet ratios of the meth-HA/meth-SF gels can be considered as relatively low, thus the gelation mechanism can be mainly attributed to vinyl–vinyl linkages, rather than the β-sheet formation between the meth-SF chains.

Another important point is that at the highest MD, while DMAA concentration does not affect the XRD patterns of the hydrogels (Figure 2c-ii), at the lowest MD, increasing DMAA concentration makes the diffraction peaks more explicit (Figure 2c-i). That is, the monomer concentration is an important parameter effecting the gel formation, especially when the MD of the meth-HA is low. To note that, these findings are also in a good accord with the W_g values of the hydrogels, because a meth-HA/meth-SF hydrogel cannot be fabricated at the lowest MD and in the absence of a monomer, whereas that's of can be fabricated with a W_g of 1 with increasing MD and monomer concentrations.

We also evaluated these results with the visual appearance and the mechanical properties of the hydrogels: Since the β-sheet crystallites create physical crosslink points that scatter the light, hydrogels with high β-sheet amounts (larger than ≈35%) generally seems completely white.[27,31–33] These crosslinks also increase the modulus of the hydrogels via increasing the efficient crosslink density, thus effecting the mechanical performances of the hydrogels.[27] Therefore, we also paraphrased our results with these perspectives to support the XRD and W_g results. Figure 2d gives Young's modulus (E)-compressibility chart of the meth-HA/meth-SF hydrogels prepared in this study together with two references given for comparison, while the Figure 2e shows the digital photographs of three of them synthesized without a monomer and in the presence of VP and DMAA monomers. Oral et al. reported a completely white meth-SF hydrogel possessing Young's modulus (E) of 265 ± 47 kPa and compressibility of about 40% with a β-sheet amount of 63 ± 1%.[27] Similarly, Tavsanli et al. also prepared a fully white meth-HA/SF hydrogel with an E and compressibility of 81 ± 11 kPa and 70% with high β-sheet content.[34] On the other hand, meth-HA/meth-SF hydrogels prepared in this study have E between 0.94 ± 0.21 and 49 ± 3 kPa, and their compressibility varies up to 95%. In addition, they are almost fully transparent, independent from the existence of a monomer or its type. Consequently, their relatively low E values and transparent morphologies support the XRD results showing the limited β-sheet amounts of the hydrogels. We should note that the β-sheet content of the hydrogels could not be determined via peak deconvolution of the amide-I band using FTIR technique because of the overlap of the β-sheet peak at 1620 cm^{-1} with the characteristic peaks of both HA and DMAA components.[27,34]

To note that, high β-sheet content in a SF-based hydrogel generally causes low toughness and brittleness in tension and compression, as shown in Figure 2d and also reported before.[35,36] Moreover, Su et al. introduced a strategy for restricting the β-sheet nucleation on purpose to fabricate mechanically durable SF-based hydrogels.[37] As a result, the given meth-HA/meth-SF hydrogels in the present study with low β-sheet contents thus can be stretched up to 300% and compressed up to 95% whose results will be discussed in the following paragraphs.

A possible explanation for the relatively low β-sheet contents of the hydrogels might be the chemically interconnected (via vinyl–vinyl linkages) thus highly entangled organization of the meth-HA and meth-SF molecules: The entanglement of such large molecules prevents the close physical interactions that occurred between the large hydrophobic parts of the meth-SF chains to be aligned to form β-sheet crystallites; thus, the main crosslink density of the hydrogels is originated from the vinyl–vinyl linkages. Moreover, due to the β-sheet nucleation takes longer than the vinyl–vinyl bond formation,[27] once the vinyl conjoining first occur, highly entangled meth-HA and meth-SF network inevitably contains interrupted chains between the hydrophobic parts of the meth-SF, and β-sheet formation cannot take place further. Besides, β-sheet formation generally requires high temperature and low pH values,[38] which not fits to our system. To note that, collagen, that is, the main protein component of the ECM, also is mainly found in helical (triple-helical structure) morphology rather than aligned crystallites in the ECM, providing a highly elastic and tough gel-like material.[39,40]

2.2. Effects of the Monomer Type on the Properties of the Hydrogels

VP and DMAA monomers at 3 w/v% concentration were introduced to meth-HA/meth-SF system, to see the effects of the monomer type on the main properties of the hydrogels. First, we performed unidirectional compression tests to see the mechanical properties of the hydrogels. Then, swelling tests were conducted, and the weight and volume swelling ratios of the hydrogels were determined as a function of MD and the monomer type. **Figure 3**a,b gives the compressive stress–strain curves of the hydrogels, and their mechanical properties such as Young's modulus (E), efficient crosslink density (ν_e) and fracture stress (σ_f) as a function of MD. E and σ_f were determined as detailed at the Experimental Section, while ν_e was calculated by assuming the affine gel network using the following equation[41,42]

$$E = 3\vartheta_e RT \quad (1)$$

where RT is the thermal energy, that is, R is the universal gas constant and T is the absolute temperature.

As mentioned above, at the lowest MD (4%), meth-HA/meth-SF hydrogels cannot be generated, in the absence of a monomer. Above the MD of 4%, a series of meth-HA/meth-SF hydrogels are obtained, whose Young's modulus (E) increase from 0.94 ± 0.21 to 3.7 ± 0.4 kPa while the fracture stresses (σ_f) decrease from 1.6 ± 0.4 to 0.39 ± 0.07 MPa, with increasing MD (Figure 3b-i,iii). On the other hand, when a monomer is integrated into the meth-HA/meth-SF system, we are both able to prepare a hydrogel at % 4 MD and adjust the mechanical properties significantly. For instance, if VP is used, the ultimate stress and strain dramatically decrease as compared to control group (Figure 3a-ii) even though an increase is observed in Young's modulus and crosslink densities (Figure 3b-i,ii). To give an example, at the MD of 8%, meth-HA/meth-SF hydrogel in the absence of VP can be compressed up to 95 ± 2% strain and 1.6 ± 0.4 MPa stress. However, its VP-including counterpart can only be compressed up to strain and stress values of about 75 ± 2% and 0.32 ± 0.04 MPa, respectively,

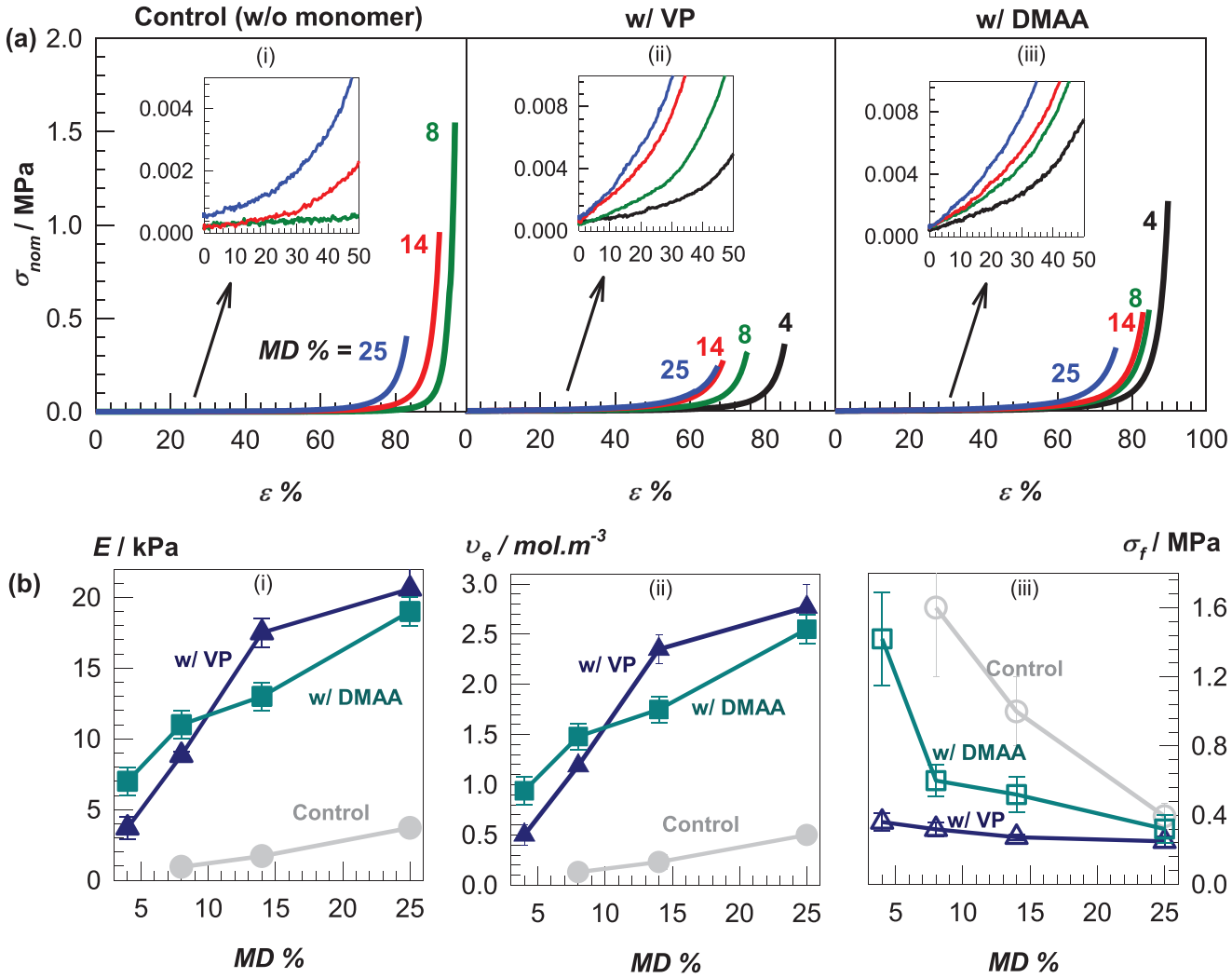

Figure 3. a) Compression stress–strain curves of the meth-HA/meth-SF hydrogels prepared in the absence of a monomer (control) and together with VP and DMAA monomers, as indicated. b) Young's modulus (E), efficient crosslink densities (ν_e), and fracture stress (σ_f) plotted against the MD.

while its E increases about ninefold. On the other hand, when DMAA is introduced to the system substituted for VP, ultimate stress and strains start to increase again and get closer to the control group showing that the DMAA is a better candidate than VP as a spacer monomer. We attributed this finding to the existence of both hydrophobic and hydrogen-bonding interactions acting as physical crosslinks when DMAA is used,[28] which are absent in the VP-included hydrogels due to the steric hindrance of the poly(VP) chains.[43]

In addition to mechanical properties, swelling abilities (q_w, q_v, m_{rel}, and V_{rel}) of the hydrogels were also determined, and they are given in **Figure 4** as a function of MD. Due to the higher Young's modulus (E), that is, crosslink density, which was obtained by the addition of a monomer and increasing in MD (Figure 3b-ii), both weight and volume swelling ratios of the monomer-included hydrogels are more below than the control group, which are also inversely proportional to the MD. For instance, m_{rel}, that is, weight swelling ratio calculated with respect to as-prepared state, of a meth-HA/meth-SF hydrogel prepared in the absence of a monomer was 14 ± 2, at MD = 25%. However, when DMAA or VP was introduced to this system, m_{rel} dramatically decreased down to 2.9 ± 0.1 and 1.4 ± 0.1 for DMAA and VP, respectively, since the crosslink density of the hydrogels are increased from 0.5 ± 0.1 to 2.55 ± 0.14 and 2.77 ± 0.23 mol m^{-3} with the addition of DMAA and VP, respectively.

2.3. Effects of the Monomer Concentration on the Properties of the Hydrogels

After the monomer type analysis, we chose DMAA monomer for further studies due to its better collaboration with the meth-HA/meth-SF system in accordance with the mechanical performances (Figure 3), and we changed its concentration from 3 to 15 w/v%. Thus, a series of meth-HA/meth-SF/DMAA hydrogels were fabricated, and then elaborately characterized: In order to see the viscoelastic properties, frequency ω sweep tests were first done at 25 °C and at a single strain amplitude γ_0 of 1%. We also

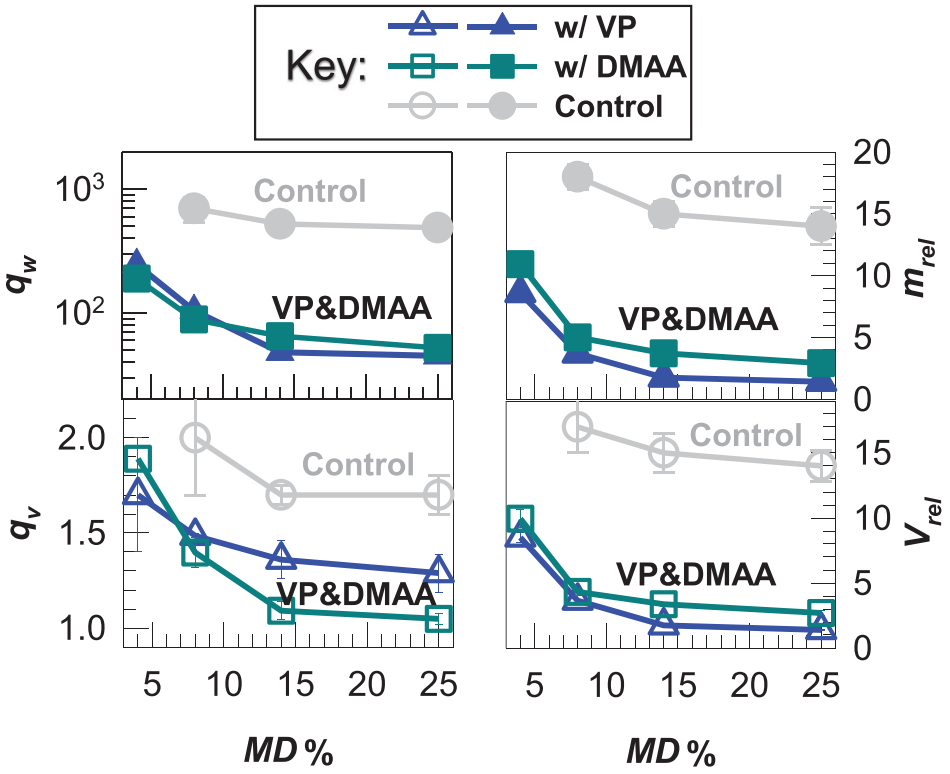

Figure 4. Weight and volume swelling ratios calculated with respect to dry (q_w and q_v), and as-prepared states (m_{rel} and V_{rel}) as a function of the MD.

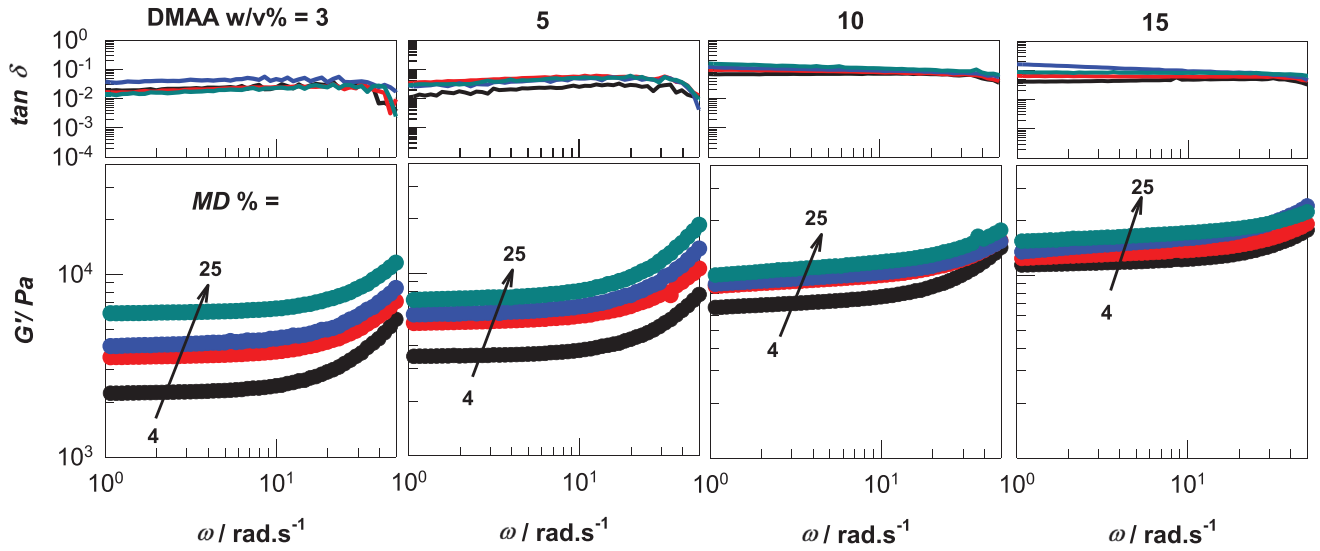

Figure 5. Frequency dependency of the G' and tan δ values of the hydrogels synthesized at various DMAA concentrations and MD.

conducted unidirectional compression and tensile tests to see the mechanical endurance of the materials. Then, cyclic compression tests were performed and fatigue resistance of the hydrogels were determined. Finally, synthesized hydrogels were immersed into water, and their swelling capacities were determined as a function of DMAA concentration.

Figure 5 gives the G' and tan δ (G''/G') values between the frequencies ω from 1 to 50 rad s^{-1} for the hydrogels prepared at various DMAA concentrations and MD ratios. Although hydrogels have an almost ω-independent nature until about 10 rad s^{-1}, their G' tends to increase above this frequency; thus, all hydrogels become ω-dependent with increasing ω. Moreover, hydrogels become less ω-dependent with increasing DMAA concentration and MD values, that is, with increasing crosslink density. These characteristic behaviors can be attributed to following facts; 1) physical entanglements, 2) relaxation times of the chains. First,

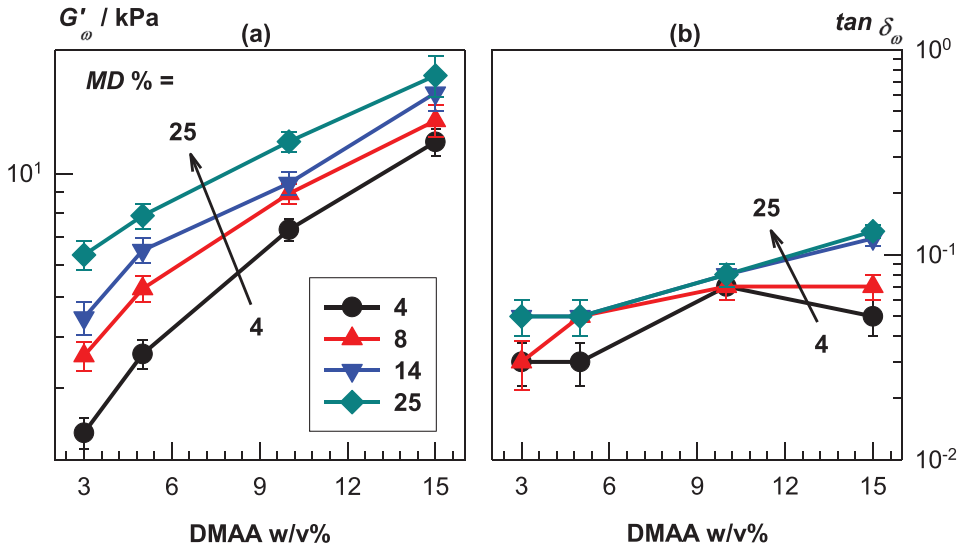

Figure 6. a) G' and b) tan δ values of a single frequency (6.28 rad s^{-1}), that is, G'_{ω} and tan δ_{ω}, as a function of DMAA concentration. MD ratios are indicated.

as meth-HA and meth-SF are large molecules, they can form physical entanglements acting as a crosslinker increasing the crosslink density thus the modulus, at very short experimental time intervals, that is, high frequencies, on account of the life times of these entanglements. As a result, modulus of the hydrogels tends to increase with increasing frequency. On the other hand, chain segments between the crosslink points are longer in loosely-crosslinked networks such as hydrogels prepared at lower DMAA concentrations and MD values, which requires longer relaxation times. On the contrary, for the highly crosslinked gel networks, the chain segments between the crosslink points are relatively smaller, whose relaxation times thus are shorter.[44,45] Therefore, hydrogels prepared at lower DMAA concentrations and MD values, that is, possessing smaller crosslink densities, exhibit larger ω-dependency as compared to hydrogels with high crosslink densities. Because, longer chains between the crosslink points do not have enough time to rearrange themselves at high frequencies, that is, short time scales, a sharp increase in G' is observed, that is, they tighten up. Hydrogels with high crosslink densities needs much higher frequencies for this kind of stiffening as the short polymer chains between the crosslink points can rearrange themselves in this frequency range. This is the main reason for the hydrogels fabricated at higher DMAA concentrations and MD values exhibit lower ω-dependency between 1 and 50 rad s^{-1} as compared to other ones. Frequency-dependent viscoelasticity is also observed in some biological molecules and systems. For instance, Palmer et al. showed that the G' of the actin networks in the cytoskeleton increases with increasing frequency with a constant high-frequency exponent of 0.78 ± 0.10.[46] Similarly, muscle cells and kidney epithelial cells also have a frequency-dependent G' values, which increases with increasing ω.[47]

To reveal the effects of the DMAA concentration on the viscoelastic properties of the hydrogels clearly, G'_{ω} and tan δ_{ω}, which are the types of the G' and tan δ that specified at a single frequency of 6.28 rad s^{-1} (1 Hz), are plotted against the DMAA concentration in **Figure 6**a,b, respectively. It is explicitly seen that G'_{ω} and tan δ_{ω} increase with increasing DMAA concentration. For example, for a hydrogel prepared at the highest MD (25%), G'_{ω} and tan δ_{ω} are 6.3 ± 0.5 kPa and 0.05 ± 0.01 when it contains 3 w/v% DMAA. After its DMAA concentration increases to 15 w/v%, these values also increase up to 18 ± 2 kPa and 0.13 ± 0.01, respectively. tan δ indicates the correlation between the elastic and viscous portions in a material, representing the stored (non-dissipated) and the lost (dissipated) energy fractions, respectively. Therefore, it can be claimed that a material with a higher tan δ has a more prominent viscous character, and it can dissipate much more energy than that of a material with a lower tan δ. From this general consideration, we can conclude that the meth-HA/meth-SF hydrogels become generally more energy dissipative while their DMAA concentrations increase (Figure 6b). To note that, these findings are also supported with energy dissipation coefficients μ of the hydrogels, which are discussed in the following paragraphs.

Figure 7a,b give the stress–strain curves of compression and tensile tests, respectively, for meth-HA/meth-SF hydrogels prepared at various DMAA concentrations and MD values as indicated. Hydrogels can be compressed up to 95% strain and 4 MPa stress depending on the MD ratio and DMAA concentration. For instance, at a constant DMAA concentration of 3 w/v%, compressibility of the hydrogels decreased with increasing MD (Figure 7a-i): A hydrogel prepared at a MD of 4% can be compressed up to 90 ± 2% corresponding to a stress value of 1.4 ± 0.3 MPa while that's of about 75 ± 2% and 0.32 ± 0.08 MPa, respectively, when MD is increased to 25%. Similarly, their stretchability also decreases about threefold (290 ± 10 vs 100 ± 8%) if the MD is increased from 4% to 25% (Figure 7b-i). DMAA concentration also affects the mechanical properties significantly likewise the MD, as summarized in **Figure 8**.

For instance, at the lowest MD (4%), E increases from 7 ± 1 to 36 ± 3 kPa, corresponding to an increase in the efficient crosslink density (ν_e) from 0.94 ± 0.14 to 4.84 ± 0.40 mol m^{-3}, when the

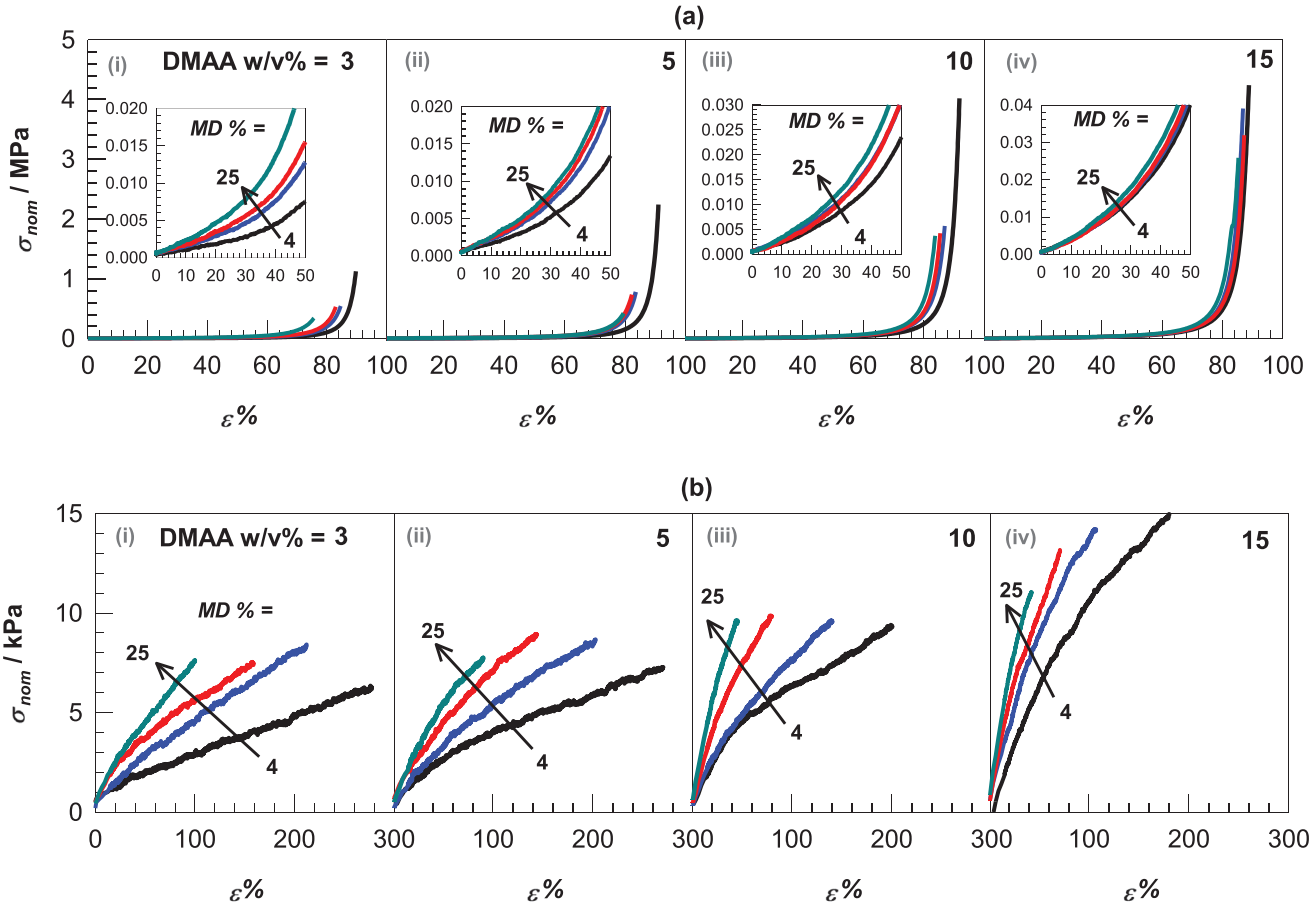

Figure 7. a) Compression and b) tensile stress–strain curves of the meth-HA/meth-SF hydrogels prepared at various DMAA concentrations (i→iv) and MD.

DMAA concentration increases from 3 to 15 w/v% (Figure 8a). Likewise, the fracture stresses (σ_f) in the compression and tensile tests increase from 1.4 ± 0.3 to 4.2 ± 0.9 MPa and from 6 ± 1 to 15 ± 3 kPa, respectively (Figure 8b). On the other hand, fracture strains in the compression and tensile tests, that is, compressibility and stretchability, decrease with increasing DMAA concentration likewise the MD ratio as mentioned above, as a result of the increasing efficient crosslink density (ν_e). To give an example, at the same MD (4%), hydrogel containing 3% DMAA can be compressed and stretched up to 90 ± 2 and 290 ± 10%, while that is about 88 ± 2 and 175 ± 9% for a hydrogel prepared at 15% DMAA, respectively. Similar trends are also observed for other MD ratios, as given in Figure 7, and summarized in Figure 8a,b. Moreover, Figure 8c shows the real-time digital photographs of a hydrogel prepared at the lowest DMAA concentration and MD, that is, 3 w/v% and 4% respectively, under compression and tensile tests.

To analyze the mechanical properties of the hydrogels with respect to toughness, the energy to break W (toughness) was determined from the area under the tensile stress–strain curves before the fracture. Figure S1, Supporting Information gives the toughness W of the hydrogels as a function of DMAA concentration and MD values as indicated. With increasing MD, W of the hydrogels significantly decreases due to the decrease in compressibility and stretchability ratios as shown in Figure 7. On the other hand, W tends to increase at the lowest MD value (4%) with increasing DMAA concentration. However, the toughness W of the hydrogels fabricated at higher MD values slightly decreases with increasing DMAA concentration.

Fatigue resistance and the energy dissipation mechanisms of the hydrogels were determined through the cyclic compression tests. Figure S2, Supporting Information gives the loading (straight lines) and unloading (dashed lines) stress–strain curves of the hydrogels. For the sake of clarity, only the first and the last (fifth) cycles are shown in these graphs. The area between the loading and unloading curves corresponds to a mechanical energy quantity called hysteresis energy U_{hys} calculated via the Equation (2a), referred to a chemical and/or physical bond breakage during deformation. Hydrogels prepared at lower DMAA concentrations (3 and 5 w/v%) possess almost no hysteresis indicating that they are nearly pure elastic materials up to 60% compression. On the other hand, hysteresis become almost visible at higher DMAA concentrations (10 and 15 w/v%) (Figure S2, Supporting Information). This may be explained via the efficient crosslink densities (ν_e) of the hydrogels. That is, ν_e significantly increased with increasing DMAA concentration, as previously shown in Figure 8a. Therefore, the more hydrogels have DMAA, the more they are stiff and highly cross-linked; thus, they possess

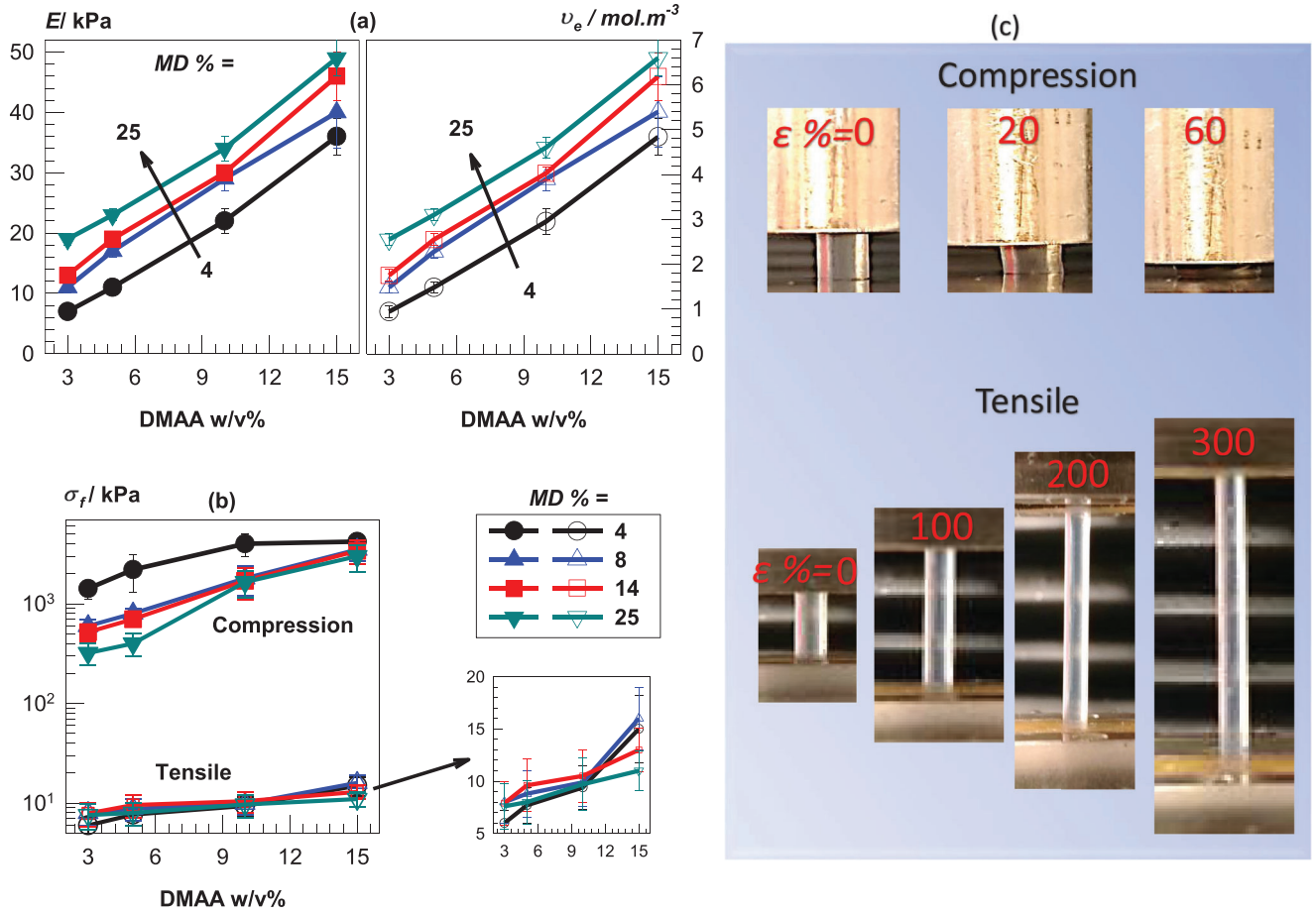

Figure 8. a) Young's modulus (E), efficient crosslink densities (ν_e) and b) fracture stresses (σ_f) of the hydrogels as a function of DMAA concentration. c) Digital photographs of a meth-HA/meth-SF hydrogel containing 3 w/v% DMAA (MD = 4%), which were taken during the compression and tensile tests at different strains as indicated.

more bonds between the crosslinking points to be disrupted, and an apparent hysteresis is obtained.

Hysteresis energies U_{hys} are also related to dissipated energy during deformation. To clarify the quantity of the dissipated energy per each loading step, we calculated the energy dissipation coefficient μ by using Equation (2b). In **Figure 9**a, U_{hys} and μ are plotted against the cycle number, also as a function of DMAA and MD, as indicated. As mentioned above, U_{hys} increase with increasing DMAA concentration, but almost independent from the cycle number, as can be seen in the upper section of Figure 9a. Similarly, it is also seen that the μ is also nearly cycle number-independent, and it is also directly proportional with DMAA concentration (bottom section of Figure 9a).

For a more understandable comparison, we calculated their arithmetical average values for all cycles, that is, $U_{hys,avg}$, and μ_{avg}, and plotted them against the DMAA concentration in Figure 9b: Average hysteresis energies $U_{hys,avg}$ were 0.37 ± 0.03 and 2.7 ± 0.5 kJ m^{-3} for the hydrogels containing 3 and 15 w/v% DMAA, respectively, at MD = 25%, showing an obvious increasing with increasing DMAA concentration. A similar step-up trend was also observed for other hydrogels prepared at the MD of 4%, 8%, and 14%. In a similar manner, μ_{avg} also increases with increasing DMAA concentration as can be given in the bottom section of Figure 9b. For example, μ_{avg} was 0.051 ± 0.001 at DMAA = 3 w/v%, while it is increased up to 0.13 ± 0.01 at a DMAA concentration of 15 w/v% when MD is 25%. To note that, in contrast to $U_{hys,avg}$, μ_{avg} also possess a noteworthy dependency to MD. Whereas the μ_{avg} varied between 0.051 and 0.13 at the highest MD (25%) as mentioned at the previous sentence, that was determined between 0.13 ± 0.01 and 0.17 ± 0.01 at the lowest MD (4%) depending on the DMAA concentration. These findings clearly imply that the hydrogels prepared at lower MD's can dissipate the mechanical energy much more efficiently than that of prepared at higher MD's. On the other hand, this energy-dissipative behavior rather increases with increasing DMAA amount due to the direct proportion between the μ_{avg} and DMAA concentration, harmonizing the DMAA-dependencies of the tan δ_ω as mentioned above.

Due to the low hysteresis (≈0.3–3 kJ m^{-3}) obtained from the five successive cyclic tests conducted up to a maximum strain ϵ_{max} of 60%, we also performed stepwise cyclic tests (ϵ_{max} = 20%, 40%, 60%, and 80%) for a chosen DMAA concentration (15 w/v%), in which the materials are gradually damaged (**Figure 10**). Step-by-step deformations create much hysteresis that increases with increasing ϵ_{max} and MD. For instance, at the lowest and the

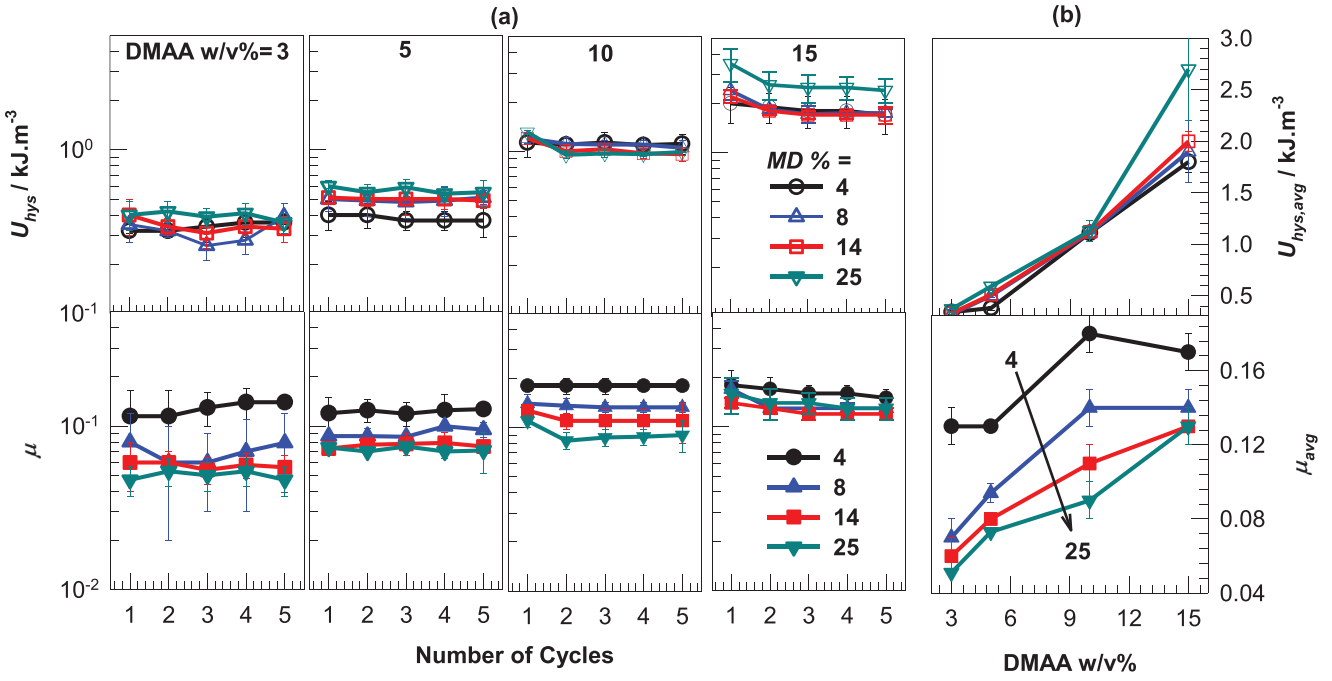

Figure 9. a) U_{hys} and μ values of the hydrogels as a function of the cycle number. b) $U_{hys,avg}$, and μ_{avg} values plotted against the DMAA concentration.

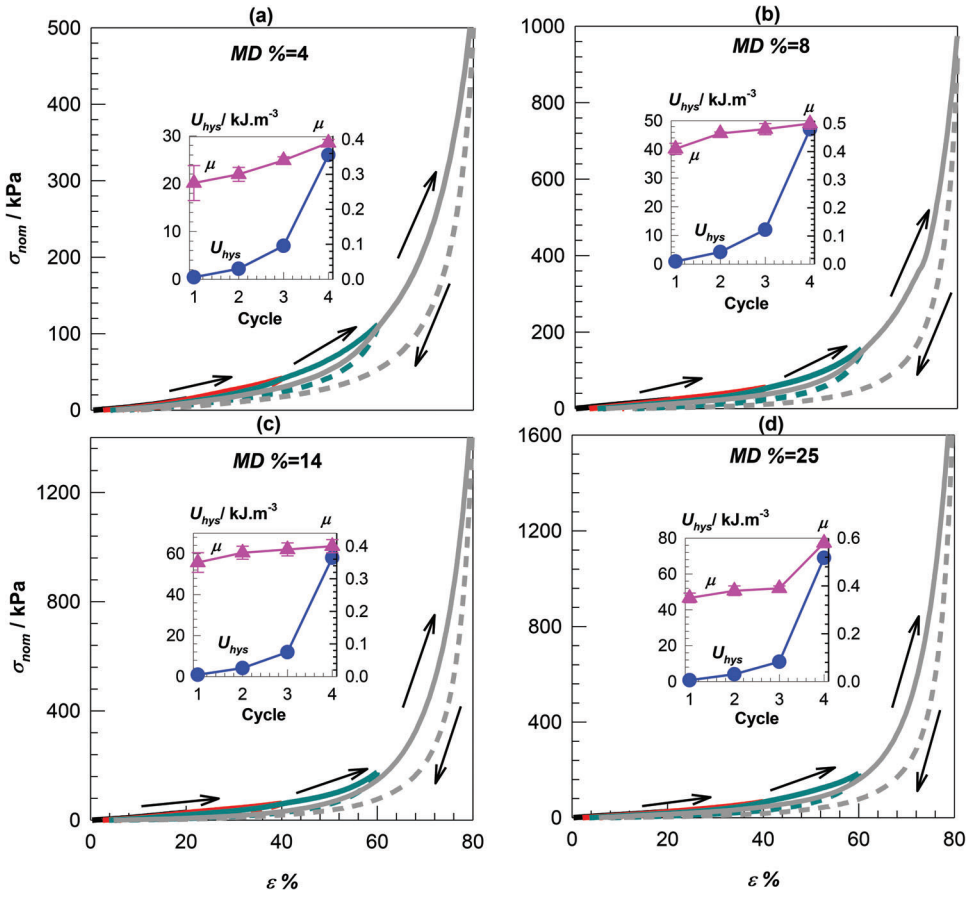

Figure 10. Stepwise cyclic tests of the hydrogels synthesized at MD of a) 4%, b) 8%, c) 14%, and d) 25%. DMAA = 15 w/v%.

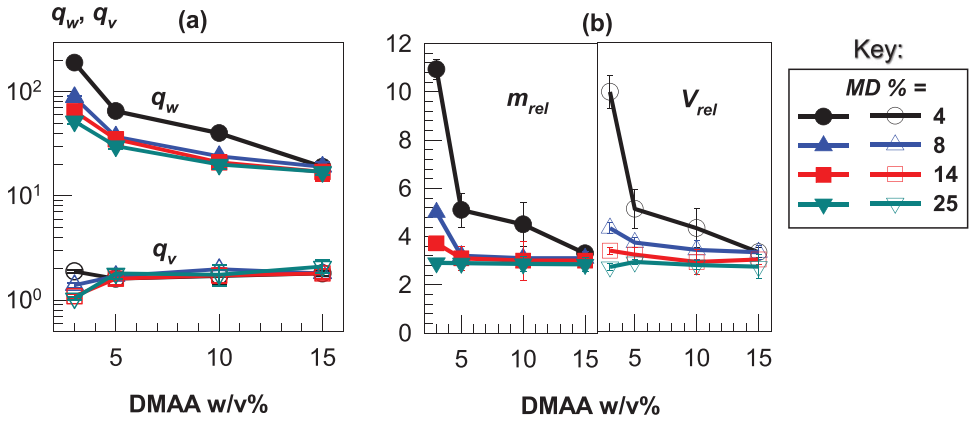

Figure 11. Weight and volume swelling ratios calculated with respect to a) dry (q_w and q_v) and b) as-prepared states (m_{rel} and V_{rel}), as a function of DMAA concentration.

highest MD values (4 and 25%), U_{hys} increases from 0.42 ± 0.05 to 26 ± 1 kJ m^{-3} and from 0.74 ± 0.02 to 69 ± 2 kJ m$^{-3,}$ respectively, with increasing cycle number, that is, ϵ_{max} (Figure 10a,d). Their μ values vary between 0.3–0.4 and 0.4–0.6, respectively, also increasing with increasing ϵ_{max} (cycle). Similar trends are also observed for other hydrogels with different U_{hys} and μ values (Figure 10b,c).

Finally, swelling properties of the hydrogels were determined, whose results are summarized in Figure 11: q_w of the hydrogels decreased from 10^2 to 10^1 range with increasing DMAA concentration, while their q_v values vary between 1 and 2, nearly independent from the DMAA concentration and MD (**Figure 11**a). On the other hand, m_{rel} and V_{rel} of the hydrogels are almost the same, and they also decrease with increasing DMAA concentration and MD due to the increasing efficient crosslink density (ν_e). The large difference observed between the q_w and q_v of the hydrogels given in both Figures 4,11 is attributed to drying method. That is, hydrogels were dried by using a freeze-dryer, which creates large pores in place of the water removed, likewise the macroporous cryogels reported before possessing large difference between the q_w and q_v due to their porosities.[22,31–33]

3. Conclusion

ECM-like soft materials have always been demanded for tissue engineering applications. Here, we reported ECM-inspired soft hydrogels of high compressibility and stretchability. These hydrogels were formed using methacrylated versions of the HA and SF, that is, meth-HA and meth-SF, as a GAG and protein component to mimic the ECM structure. Meth-HA/meth-SF hydrogels were fabricated both in the absence and in the presence of a monomer such as DMAA or VP, in which the meth-HA and meth-SF act as a macromer and a macrocrosslinker, respectively. Meth-HA/meth-SF hydrogels without a monomer had Young's modulus (E) varied between 0.94 ± 0.21 and 3.7 ± 0.4 kPa, depending on the MD. With the addition of a monomer, E was increased from 3.7 ± 0.4 to 49 ± 3 kPa as a function of MD and monomer type and concentration. These E, and corresponding crosslink density (ν_e) values, lower than the order of ≈10^2 kPa and ≈10^1 mol m^{-3} together with the XRD measurements showed that the meth-SF is mainly found in randomly coiled and/or helical conformations rather than the β-sheet crystallites in the hydrogels, providing the high compressibility and stretchability. This conformational organization, that is, the interwoven polymer chains rather than the brittle crystallites, also provided the fatigue resistance. For instance, DMAA-included hydrogels showed very low hysteresis (between ≈0.3 to 3 kJ m^{-3}) after five successive cyclic compression tests conducted up to 60% strain. Besides, they showed highly frequency-dependent viscoelastic nature above 10 rad s^{-1}, likewise some cells and biological molecules. It is believed that as-prepared meth-HA/meth-SF hydrogels with tunable properties will be good candidates for soft tissue engineering applications. Furthermore, hydrogels reported here may also be suitable for other applications such as soft robotics where soft but tough and non-brittle materials are required rather than the rigid and the hard ones to increase the locomotion and the capability of the mobility of the robotic components and other smart adaptive devices. To conclude, the method developed in this study might be useful for other protein or carbohydrate biopolymers that can be chemically modified and then crosslinked via spacer monomer segments to fabricate high toughness hydrogels with adjustable viscoelastic properties.

4. Experimental Section

Materials: SF protein was isolated from domesticated *Bombyx Mori* silkworm cocoons purchased from Bursa Kozabirlik in Turkey. Na_2CO_3 and LiBr (both Merck) were used without any purification. HA sodium salt (Sigma Aldrich) from *Streptococcus equi* (M_w = 1.2 × 10^6 g mol^{-1}),[48] DMAA (Sigma Aldrich), VP (Sigma Aldrich), glycidyl methacrylate (GM, Sigma Aldrich), tetrabutylammonium bromide (TBAB, Sigma Aldrich, ≥99%), triethylamine (TEA, Merck), acetone (Tekkim, 99.5%), and Irgacure 2959 were also used as received.

Methacrylation of HA and SF: Methacrylation of the HA and SF and the determination of their methacrylation degrees MD were achieved as detailed before.[26–28] Briefly, in order to methacrylate the HA, 0.5 g of it was dissolved in 50 mL distilled water at room temperature. Then, GM, TEA, and TBAB were added to HA solution to methacrylation of the HA. For instance, to prepare a solution containing sixfold molar excess of GM with respect to the disaccharide repeat unit of HA, 1 mL of GM, 1 mL of TEA, and 1 g of TBAB were added. After heating the solution to 55 °C and stirring for 1 h, it was cooled down to room temperature and precipitated in acetone. Finally, the precipitate was dissolved in water, and the obtained

solution of methacrylated HA (meth-HA) was freeze-dried for further usage. MD of the meth-HA was varied as 4%, 8%, 14%, and 25%, determined as reported before.[28]

On the other hand, 10 g *B. mori* silkworm cocoons were cut into two pieces to remove the silkworms inside the cocoons, and they were washed with distilled water several times. Then, they were transferred into 0.02 M aqueous Na_2CO_3 solution (1 L) and boiled for 1 h to remove sericin protein. After isolation, SF moved from Na_2CO_3 solution was washed away with distilled water (70 °C) 5 times, each for 20 min. After drying at room temperature, 7 g of SF was dissolved in 35 mL aqueous 9.3 M LiBr solution at 60 °C at 250 rpm. After dissolution taking place for about 1 h, 2 mL of GM was added, and the stirring was continued at the same temperature for a further 3 h at 500 rpm to methacrylation. Finally, the solution was put into a dialysis tube (10 000 MWCO, Snake Skin, Pierce) and dialyzed against distilled water for 4 days to distract the LiBr and unreacted GM, and to finally obtain an aqueous methacrylated SF (meth-SF) solution, whose concentration was gravimetrically determined and fixed at 5 w/v% for the entire study. Methacrylation degree of the meth-SF was fixed at 14%, which was determined as reported before.[27]

Synthesis of the Hydrogels: After the methacrylation of the HA and SF at four (4%, 8%, 14%, and 25%) and one (14%) methacrylation degrees MD, respectively, they were utilized for the preparations of the hydrogels. In this study, three series of hydrogels were prepared by using Irgacure 2959 initiator in a UV reactor, at room temperature. First, meth-HA/meth-SF hydrogels in the absence of a vinyl monomer were synthesized as a control group. For this, the meth-HA and meth-SF concentrations were fixed at 1 and 2.5 w/v%, respectively, while the UV initiator was 2.2% by weight regarding total meth-HA/meth-SF amount (Series 1). Then, two different vinyl monomers (DMAA or VP) were separately introduced at 3 w/v% concentrations to aforementioned meth-HA/meth-SF mixture to be acted as a dual macrocrosslinker system to reveal the effects of the monomer type (Series 2). Finally, the DMAA was chosen for further synthesis and increased its concentration from 3 to 15 w/v% (Series 3), thus fabricated a series of meth-HA/meth-SF/DMAA hydrogels whose characterizations were comprehensively performed.

Typically, a meth-HA/meth-SF hydrogel containing 3 w/v% DMAA was prepared by the following route: 0.1 g of meth-HA prepared at various MDs were first dissolved in 4.69 mL of water overnight via stirring at 100 rpm. Then, 5 mL meth-SF solution (5 w/v%) was added drop by drop to the meth-HA solutions. Finally, 0.31 mL (0.30 g) DMAA and 7.7 mg Irgacure 2959 were added, and the mixtures were stirred until obtaining homogeneous reaction solutions of 10 mL total volume. Solutions were then molded within several plastic syringes of various diameters to obtain cylindrical gel specimens by exposing them to UV irradiation at 365 nm for 24 h.

Characterization of the Hydrogels: Hydrogel specimens ejected from the syringes were cut into small pieces for characterizations. Frequency sweep tests were conducted using a Bohlin Gemini 150 model rheometer system equipped with a parallel plate of 20 mm in diameter. Gel specimens possessing the same diameter as the measuring plate were placed in the rheometer until the gap size became 2.0 ± 0.2 mm. Finally, elastic modulus G', viscous modulus G'', and loss factor tan δ (G''/G') were monitored as a function of the frequency ω while the strain amplitude γ_0 was fixed at 1%.

Unidirectional compression and tensile tests were applied at room temperature at a strain rate of 1.7 min^{-1} using a Zwick Roell Z0.5 TH mechanical test machine with a 500 N load cell to obtain nominal stress (σ_{nom})–strain (ϵ) curves. The Young's modulus (E) was determined via 5–15% strain interval while the fracture stresses (σ_f) were calculated through the maxima of the σ_{nom}–ϵ curves as detailed before.[49] In addition, two different sets of cyclic compression tests, that is, loading–unloading tests, were carried out to reveal the fatigue resistance of the hydrogels at the same conditions. In the first set, that is, the one-step cyclic tests, five successive loading and unloading tests were performed up to a constant ϵ_{max} of 60%. In the second set, that is, the stepwise cyclic tests, four successive loading and unloading tests were done, in which ϵ_{max} was increased from 20% to 80% step-by-step for each cycle. To note that, there was no holding time between the cycles. Cyclic tests provided the calculations of the hysteresis energies (U_{hys}) and the energy dissipation coefficients (μ), which indicate the energy difference between the loading–unloading curves and the amount of the loading energy that dissipated, respectively. They were calculated by using the following equations[50]

$$U_{hys} = \int_0^{\epsilon_{max}} \sigma_{nom} d\varepsilon - \int_{\epsilon_{max}}^0 \sigma_{nom} d\varepsilon \tag{2a}$$

$$\mu = \frac{U_{hys}}{\int_0^{\epsilon_{max}} \sigma_{nom} d\varepsilon} \tag{2b}$$

where ϵ_{max} was equal to 60% in one-step cyclic tests, and it was 20%, 40%, 60%, and 80% in stepwise cyclic tests. Since it was found out that the U_{hys} and μ do not change much with cycle number in one-step cyclic tests, their arithmetical average values were calculated, that is, $U_{hys,avg}$ and μ_{avg}, respectively, in order to exhibit the effect of the DMAA concentration more clearly. For this, the following equations were used

$$U_{hys,avg} = \frac{\sum_{i=1}^{5} U_{hys,i}}{5} \tag{3a}$$

$$\mu_{avg} = \frac{\sum_{i=1}^{5} \mu_i}{5} \tag{3b}$$

where i is the number of cycles.

For swelling and extraction studies, hydrogels were put into distilled water until swelling equilibrium, and their weight (q_w, m_{rel}) and volume (q_v, V_{rel}) swelling ratios in addition to gel fractions (W_g) were calculated as[28,51]

$$q_w = \frac{m_s}{m_d} \tag{4a}$$

$$m_{rel} = \frac{m_s}{m_0} \tag{4b}$$

$$q_v = \left(\frac{D_s}{D_d}\right)^3 \tag{5a}$$

$$V_{rel} = \left(\frac{D_s}{D_0}\right)^3 \tag{5b}$$

$$W_g = \frac{m_d}{cm_0} \tag{6}$$

where the subscripts of *s, d*, and 0 indicate the swollen, dried, and as-prepared states, respectively, while the m, D, and c are the masses, diameters, and the total met-HA/meth-SF/monomer concentrations of the hydrogels.

Finally, XRD measurements were performed on dry gel samples in powder state by using a PANalytical X-Pert PRO Multi-Purpose Diffractometer using Ni-filtered CuKα ($\lambda = 0.15418$ nm) radiation at 45 kV and 40 mA in the range of $2\theta = 5$–40°. Baseline corrections of the XRD data were performed by using PeakFit Software (Version 4.12, SeaSolve Software Inc.).

Supporting Information

Supporting Information is available from the Wiley Online Library or from the author.

Acknowledgements

O.O. thanks the Turkish Academy of Sciences (TUBA) for the partial support.

Conflict of Interest

The authors declare no conflict of interest.

Data Availability Statement

The data that support the findings of this study are available in the Supporting Information of this article.

Keywords

extracellular matrix, hyaluronic acid, hydrogels, silk fibroin

Received: May 16, 2022
Revised: June 27, 2022
Published online:

[1] F. Burla, Y. Mulla, B. E. Vos, A. Aufderhorst-Roberts, G. H. Koenderink, *Nat. Rev. Phys.* **2019**, *1*, 249.
[2] Y. Tseng, T. P. Kole, J. S. H. Lee, E. Fedorov, S. C. Almo, B. W. Schafer, D. Wirtz, *Biochem. Biophys. Res. Commun.* **2005**, *334*, 183.
[3] D. A. Fletcher, R. D. Mullins, *Nature* **2010**, *463*, 485.
[4] L. I. Smith-Mungo, H. M. Kagan, *Matrix Biol.* **1998**, *16*, 387.
[5] H. M. Kagan, W. Li, *J. Cell. Biochem.* **2003**, *88*, 660.
[6] C. Chen, J. Tang, Y. Gu, L. Liu, X. Liu, L. Deng, C. Martins, B. Sarmento, W. Cui, L. Chen, *Adv. Funct. Mater.* **2019**, *29*, 1806899.
[7] H. Liu, M. Li, C. Ouyang, T. J. Lu, F. Li, F. Xu, *Small* **2018**, *14*, 1801711.
[8] X. Du, H. Cui, T. Xu, C. Huang, Y. Wang, Q. Zhao, Y. Xu, X. Wu, *Adv. Funct. Mater.* **2020**, *30*, 1909202.
[9] M. K. Lee, M. H. Rich, J. Lee, H. Kong, *Biomaterials* **2015**, *58*, 26.
[10] P. Calvert, *Adv. Mater.* **2009**, *21*, 743.
[11] H. R. Brown, *Macromolecules* **2007**, *40*, 3815.
[12] C. Creton, *Macromolecules* **2017**, *50*, 8297.
[13] A. Nakayama, A. Kakugo, J. P. Gong, Y. Osada, M. Takai, T. Erata, S. Kawano, *Adv. Funct. Mater.* **2004**, *14*, 1124.
[14] D. C. Tuncaboylu, M. Sari, W. Oppermann, O. Okay, *Macromolecules* **2011**, *44*, 4997.
[15] A. A. Gavrilov, I. I. Potemkin, *Soft Matter* **2018**, *14*, 5098.
[16] K. Haraguchi, T. Takehisa, *Adv. Mater.* **2002**, *14*, 1120.
[17] V. R. Feig, H. Tran, M. Lee, Z. Bao, *Nat. Commun.* **2018**, *9*, 2740.
[18] J. R. E. Fraser, T. C. Laurent, U. B. G. Laurent, *J. Intern. Med.* **1997**, *242*, 27.
[19] C. Vepari, D. L. Kaplan, *Prog. Polym. Sci.* **2007**, *32*, 991.
[20] J. Melke, S. Midha, S. Ghosh, K. Ito, S. Hofmann, *Acta Biomater.* **2016**, *31*, 1.
[21] B. Kundu, R. Rajkhowa, S. C. Kundu, X. Wang, *Adv. Drug Delivery Rev.* **2013**, *65*, 457.
[22] B. Yetiskin, O. Okay, *Int. J. Biol. Macromol.* **2019**, *122*, 1279.
[23] S. Yan, Q. Zhang, J. Wang, Y. Liu, S. Lu, M. Li, D. L. Kaplan, *Acta Biomater.* **2013**, *9*, 6771.
[24] S. Yan, Q. Wang, Z. Tariq, R. You, X. Li, M. Li, Q. Zhang, *Int. J. Biol. Macromol.* **2018**, *118*, 775.
[25] J. Jaipaew, P. Wangkulangkul, J. Meesane, P. Raungrut, P. Puttawibul, *Mater. Sci. Eng. C* **2016**, *64*, 173.
[26] S. H. Kim, Y. K. Yeon, J. M. Lee, J. R. Chao, Y. J. Lee, Y. B. Seo, M. T. Sultan, O. J. Lee, J. S. Lee, S.-I Yoon, I.-S. Hong, G. Khang, S. J. Lee, J. J. Yoo, C. H. Park, *Nat. Commun.* **2018**, *9*, 1620.
[27] C. B. Oral, B. Yetiskin, O. Okay, *Int. J. Biol. Macromol.* **2020**, *161*, 1371.
[28] B. Tavsanli, O. Okay, *Eur. Polym. J.* **2017**, *94*, 185.
[29] L. Wang, Y. Zhang, Y. Xia, C. Xu, K. Meng, J. Lian, X. Zhang, J. Xu, C. Wang, B. Zhao, *Int. J. Biol. Macromol.* **2022**, *215*, 155.
[30] J. Ryoo, J. Choi, C. S. Ki, *Polymer* **2020**, *202*, 122733.
[31] F. Ak, Z. Oztoprak, I. Karakutuk, O. Okay, *Biomacromolecules* **2013**, *14*, 719.
[32] B. Yetiskin, O. Okay, *Polymer* **2017**, *112*, 61.
[33] B. Yetiskin, C. Akinci, O. Okay, *Polymer* **2017**, *128*, 47.
[34] B. Tavsanli, O. Okay, *Carbohydr. Polym.* **2019**, *208*, 413.
[35] Z. Li, Z. Zheng, Y. Yang, G. Fang, J. Yao, Z. Shao, X. Chen, *ACS Sustainable Chem. Eng.* **2016**, *4*, 1500.
[36] F. Chen, S. Lu, L. Zhu, Z. Tang, Q. Wang, G. Qin, J. Yang, G. Sun, Q. Zhang, Q. Chen, *J. Mater. Chem. B* **2019**, *7*, 1708.
[37] D. Su, M. Yao, J. Liu, Y. Zhong, X. Chen, Z. Shao, *ACS Appl. Mater. Interfaces* **2017**, *9*, 17489.
[38] A. Matsumoto, J. Chen, A. L. Collette, U.-J. Kim, G. H. Altman, P. Cebe, D. L. Kaplan, *J. Phys. Chem. B* **2006**, *110*, 21630.
[39] B. Brodsky, A. V. Persikov, *Adv. Protein Chem.* **2005**, *70*, 301.
[40] K. Rosenberg, H. Olsson, M. Mörgelin, D. Heinegård, *J. Biol. Chem.* **1998**, *273*, 20397.
[41] P. J. Flory, *Principles of Polymer Chemistry*, Cornell University Press, Ithaca **1953**.
[42] L. R. G. Treloar, *The Physics of Rubber Elasticity*, University Press, Oxford **1975**.
[43] G. Song, Z. Zhao, X. Peng, C. He, R. A. Weiss, H. Wang, *Macromolecules* **2016**, *49*, 8265.
[44] M. J. Moura, M. M. Figueiredo, M. H. Gil, *Biomacromolecules* **2007**, *8*, 3823.
[45] K. S. Anseth, C. N. Bowman, L. Brannon-Peppas, *Biomaterials* **1996**, *17*, 1647.
[46] A. Palmer, T. G. Mason, J. Xu, S. C. Kuo, D. Wirtz, *Biophys. J.* **1999**, *76*, 1063.
[47] A. Bonfanti, J. L. Kaplan, G. Charras, A. Kabla, *Soft Matter* **2020**, *16*, 6002.
[48] A. Ström, A. Larsson, O. Okay, *J. Appl. Polym. Sci.* **2015**, *132*, 42194.
[49] A. Argun, V. Can, U. Altun, O. Okay, *Macromolecules* **2014**, *47*, 6430.
[50] O. Akca, B. Yetiskin, O. Okay, *J. Appl. Polym. Sci.* **2020**, *137*, 48853.
[51] M. P. Algi, O. Okay, *Eur. Polym. J.* **2014**, *59*, 113.

